Index of supplemental information

Supplemental methods

Patient samples

These TMAs were holding 2-4 cores of 1.6 mm in diameter per tumour, dependent on the source of the material or the morphology of the tumour (two cores: biopsy; three cores: resection/excision etc; four cores: heterogeneous morphology, or separate areas of dedifferentiation). As controls and for orientation purposes, each TMA contained three cores tonsil and three cores placenta, either decalcified with EDTA or formic acid or non-decalcified.

Gene expression analysis

Normalisation and exploratory analysis of the RNA sequencing data was performed in R (v.4.0.2) by using DESeq2 (v. 1.30.1). BiomaRt (R, v.2.46.3) was used to translate the ensemble IDs to known protein coding genes. The most variably expressed genes were determined by calculating the variance per gene across all samples. The immunologic constant of rejection (ICR) gene signature was used to describe the activity state immune microenvironment and to identify distinct immune-related clusters (Th1-related markers: *IFNG*, *STAT1*, *IL12B*, *IRF1*, *TBX21*; CD8+ T cells: *CD8A*, *CD8B*; Immune effector molecules: *GZMA*, *GZMB*, *GZMH*, *PRF1*, *GNLY*; Chemokine ligands: *CXCL9*, *CXCL10*, *CCL5*; Immune suppressive molecules: *IDO1*, *PDCD1*, *CD274*, *CTLA4*, *FOXP3*) (1). The mean of the log2 normalised expression of these 20 genes was used to attribute an ICR "score" to each sample for comparison between the sarcoma subtypes, which was visualised with ggplot2 (R, v.3.3.6). For both the heatmaps in **figure 1**, a Z-Score was calculated per gene to visualise the transcriptional profile of the samples by using the Ward variance method with ComplexHeatmap (R, v.2.11.1). Differential gene expression analysis was performed with DESeq2 comparing chordomas to all other sarcomas. Genes were considered differentially expressed when the log2 fold change was above 2 and the adjusted *P* value was below 0.01. Immune-related genes were selected for visualisation in the enhanced volcano plot and additional boxplots. For visualisation purposes, the axes of the enhanced volcano plot were manually adjusted as follows: log2 fold change (x-axis) was set between -10 and 10, and the -log10 adjusted *P* (y-axis) was set to a maximum of 100.

Imaging mass cytometry analysis

To correct for variability in signal-to-noise ratios between FFPE sections, the signal intensity of the generated images was normalised at pixel levels by using Matlab (v.R2021a), after which the images were binarised using semi-automated background removal in Ilastik (v.1.3.3) as described previously (2). Probability masks were generated in Ilastik by using a multicoloured image including the DNA channel, CD45 channel, Keratin channel and Vimentin channel to annotate nucleus, cytoplasm and

background. Probability masks were loaded into CellProfiler (v.2.2.0) and used for creating cell segmentation masks. Next, the segmentation masks and binarised images were loaded into ImaCyte (3) to generate single cell-FCS files containing relative frequency of positive pixels for each marker, which were then used for phenotyping in CytoSplore (v.2.3.1) by sequentially utilizing Hierarchical Stochastic Neighbour Embedding (H-SNE) and t-distributed Stochastic Neighbour Embedding (t-SNE). Identified cell phenotypes were loaded into ImaCyte together with the segmentation masks and binarised images, which allows the mapping of the phenotypes back onto the images. Phenotypes per image were extracted to calculate the mean cell density per mm^2 for every sample (one image = one mm^2). An overview of the lineage markers used for phenotype identification is listed in **supplemental table 2**. Patients were clustered into two groups based on the Z-Score normalised mean cell densities per mm^2 of all five identified T cell phenotypes by using the Ward variance method with ComplexHeatmap. Ggplot2 was used to visualise the mean cell densities and to compare them between both T cell groups. For statistical testing, a two-sided student's t-test was performed followed by a Benjamini-Hochberg FDR correction. In addition, an overview heatmap containing all identified phenotypes in the microenvironment of chordomas was visualised with ComplexHeatmap.

Spatial interaction analysis

After phenotype calling, a spatial interaction analysis was performed with ImaCyte for all imaged samples, comparing T cell low with T cell high chordomas. ImaCyte utilises a 1000-iteration permutation test which calculates a Z-Score for the interaction between adjacent cells. However, permutation testing does not adjust for overabundant cell types, such as tumour cells, and is therefore not able to identify meaningful interactions for tumour cells. Because of the range of the calculated Z-Scores, interactions with a Z-Score below 10 were considered not significant and therefore removed for visualisation only. If an interaction Z-Score was higher than 10 in one group and lower than 10 in the other group, this interaction was considered significant for one group. When both Z-Scores were higher than 10, this interaction would be considered significant in both groups. A comparative interaction heatmap between all phenotypes excluding tumour cells was visualised with ggplot2.

Multispectral immunofluorescent imaging of T cells

All TMAs were imaged at 20x, after which the images were processed with inForm (v.2.4), which comprises background removal for each antibody by normalisation of the spectra, and analysed with QuPath (v.0.3.1). Object classification was performed by using the following classes: $CD3^+FOXP3^+$ = Regulatory T cells, $CD3^+CD8^+$ = $CD8^+$ T cells, $CD3^+$ = $CD4^+$ T cells, $CD3^+$Ki-67^+ = Proliferating T cells, CD3- = Rest. Counts per image (one image = 1 mm x 1.3 mm) were normalised per patient to counts per

mm^2 tissue. Patients were divided into a T cell high and low cluster based on the unsupervised clustering of the Z-scores of all T cell phenotypes.

Survival analysis

For all chordoma patients, Kaplan-Meier curves for the disease-specific survival and recurrence-free survival were generated with the survminer and survival packages (R, v.0.4.9 and v.3.1-12 respectively). The disease-specific survival was considered the survival of a patient until death due to the disease, whereas the recurrence-free survival was considered the time until a patient was diagnosed with a recurrence, thereby excluding patients who did not receive surgery. Since the cohort included many censored cases, the log-rank *P* value was used to estimate the significance of the associations. Known prognostic factors such as the anatomical tumour location excluding the only extra-axial patient, age and type of treatment, surgical margin excluding patients who did not receive surgery and disease recurrence were investigated for their prognostic value, as well as the newly identified T cell infiltration groups. Univariate and multivariate analyses were performed in R according to the cox proportional hazard model. Only clinical parameters that were found significant in the univariate analysis were taken along in the multivariate analysis.

TCR β-chain sequencing

The number of clones and the Shannon diversity, a measure for clonal enrichment, were calculated in R by using productive counts only, meaning that a clone needed at least 10 plus and 10 minus counts. Because recurrences showed similar levels of TCR diversity as their respective primary tumour, we used the TCR repertoire of recurrences for three patients for which there was no frozen material of primary tumours available. Finally, the data was visualised in R using ggplot2.

Supplemental table 1. Imaging mass cytometry marker panel. Ab = antibody, ON = overnight, PDPN = podoplanin.

	Target	Clone	Metal	Incubation Time	Temp	Dilution (x)
Lymphoid	CD103	EPR4166(2)	168 Er	5h	RT	50
	CD20	H1	142 Nd	Overnight	4C	100
	CD3	EP449E	153 Eu	Overnight	4C	50
	CD38	EPR4106	169 Tm	Overnight	4C	100
	CD4 + 2nd AB	EPR6855	145 Nd	Indirect ON	4C	100
	CD7	EPR4242	174 Yb	5h	RT	100
	CD8a	D8A8Y	146 Nd	5h	RT	50
	FOXP3	D608R	159 Tb	Overnight	4C	50
	TCRγδ + 2nd Ab	H41	148 Nd	Indirect ON	4C	50
Myeloid	CD11b	D6X1N	144 Nd	5h	RT	100
	CD11c	EP1347Y	176 Yb	5h	RT	100
	CD14	D7A2T	163 Dy	5h	RT	100
	CD15	MC480	171 Yb	Overnight	4C	100
	CD163	D6U1J	173 Yb	5h	RT	50
	CD204	J5HTR3	164 Dy	5h	RT	50
	CD68	D4B9C	143 Nd	Overnight	4C	100
	HLA-DR	TAL 1B5	141 Pr	5h	RT	100
Stroma	CD31	89C2	147 Sm	Overnight	4C	100
	CD39	EPR20627	157 Gd	5h	RT	100
	CD45	D9M8I	149 Sm	Overnight	4C	50
	CD45RO	UCHL1	165 Ho	Overnight	4C	100
	D2-40 (PDPN)	D2-40	166 Er	Overnight	4C	100
	TGF-β	TB21	115 In	5h	RT	100
	Vimentin	D21H3	194 Pt	Overnight	4C	50
Activation	Cleaved Caspase	5A1E	172 Yb	5h	RT	100
	Granzyme B	D6E9W	150 Nd	5h	RT	100
	ICOS	D1K2T(TM)	161 Dy	5h	RT	50
	IDO	D5J4E(TM)	162 Dy	Overnight	4C	100
	Ki-67	8D5	152 Sm	Overnight	4C	100
	LAG-3	D2G40(TM)	155 Gd	5h	RT	50
	PD-1	D4W2J	160 Gd	5h	RT	50
	PD-L1	E1L3N(R)	156 Gd	Overnight	4C	50
	Tbet	4B10	170 Er	5h	RT	50
	TIM-3	D5D5R(TM)	154 Sm	5h	RT	100
	VISTA	D1L2G(TM)	158 Gd	5h	RT	100
Tumour	CD56	E7X9M	167 Er	5h	RT	100
	CD57	HNK-1 / Leu-7	151 Eu	Overnight	4C	100
	Keratin	C11 and AE1/AE3	198 Pt	Overnight	4C	50
	P16ink4a	D3W8G	175 Lu	Overnight	4C	100
	β-Catenin	D10A8	89 Y	Overnight	4C	100
DNA	Histone H3	D1H2	209 Bi	Overnight	4C	50

Supplemental table 2. Cell type lineage markers imaging mass cytometry. Colours are indicating cell types according to overview heatmap in **supplemental figure 2**. Lineage markers are describing the used markers for cell type identification as used in this study. Lin = lineage markers e.g. CD14 and CD68.

Cell type	Lineage markers
T cells	CD3+
B cells	CD20+
Innate lymphoid cells	CD3-CD7+
Dendritic cells	CD11c+CD68- | Lin-HLA-DR+
Monocytes	CD11c-CD14+CD68-
Immune cells	CD45+
Plasma B cells	CD38+
Macrophages	CD68+
Granulocytes	CD15+
Stromal cells	Vimentin+CD45-
Vessels	CD31+
Tumour cells	Keratin+

Supplemental table 3. Top 200 most variably expressed genes across sarcoma subtypes. Known chordoma-related genes are annotated in **bold** (4-6). Genes are ordered following the heatmap presented in **figure 1A**.

Supplemental table 4. Differentially expressed genes comparing chordomas with other sarcomas. Contains the results from the differential gene expression analysis with DESeq2. Genes with a log2 fold change > 2 and an adjusted P < 0.01 were considered significantly differentially expressed. Known immune-related genes are annotated in the column "hgnc_symbol" with a yellow-filled cell. lfcSE = log fold change standard error; FDR = false discovery rate.

Supplemental table 5. Univariate cox proportional hazard results in the combined cohort. Table includes the results of the disease-specific survival in association with all identified T cell phenotypes. Log-rank *P* values < 0.05 were considered significant. * < 0 .05, ** < 0.01, *** < 0.001. HR = hazard ratio; CI = confidence interval.

	Disease-Specific Survival	
	Univariate	
Variable	**HR (95% CI)**	**log-rank P**
Ki-67+CD4+ T cells	0.93 (0.72-1.2)	0.6
Ki-67+CD8+ T cells	1 (0.9-1.1)	0.9
Ki-67+ Regulatory T cells	0.8 (0.46-1.4)	0.4
CD4+ T cells	1 (0.99-1)	0.5
CD8+ T cells	1 (0.98-1.01)	0.8
Regulatory T cells	0.95 (0.88-1.02)	0.2

Supplemental table 6. Univariate and multivariate cox proportional hazard results in the combined cohort. Table includes the results of the disease-specific, recurrence-free and metastasis-free survival. Significant parameters from the univariate analysis were taken along for the multivariable analysis. Patients who were only treated with radiotherapy were excluded from the recurrence-free survival analysis. Log-rank *P* values < 0.05 were considered significant and are annotated in bold and by significance level; * < 0 .05, ** < 0.01, *** < 0.001. HR = hazard ratio; CI = confidence interval; RT = radiotherapy.

Disease-specific survival	Univariate	
Variable	**HR (95% CI)**	**log-rank *P***
Age at diagnosis	1 (0.98-0.99)	0.2
Max tumour size	1 (0.91-1.2)	0.7
Location (Skull base)[a]		
Mobile Spine	0.56 (0.2-1.6)	0.09
Sacrococcygeal	0.35 (0.13-0.92)	
Treatment (RT alone)		
Surgery	0.87 (0.24-3.1)	0.6
Surgery + RT	**0.57 (0.15-2.2) ***	
Timing of RT (Adjuvant)[b]		
Neoadjuvant	0.66 (0.076-5.8)	0.7
Surgical margin (R0)[c]		
R1	2.1 (0.23-19)	0.3
R2	2.3 (0.75-6.8)	
T cell infiltration (High)		
Low	2 (0.78-5.3)	0.1
Disease recurrence (No)[c]		
Yes	2 (0.78-5.3)	0.9

Metastasis-free survival	Univariate	
Variable	**HR (95% CI)**	**log-rank *P***
Age at diagnosis	1 (0.99-1)	0.3
Max tumour size	1.1 (0.95-1.2)	0.3
Location (Skull base)[a]		
Mobile Spine	0.84 (0.21-3.4)	0.8
Sacrococcygeal	1.2 (0.4-4)	
Treatment (RT alone)		
Surgery	1 (0.23-5.1)	1
Surgery + RT	0.95 (0.2-4.5)	
Timing of RT (Adjuvant)[b]		
Neoadjuvant	3.6e-9 (0-Inf)	0.2
Surgical margin (R0)		
R1	2.6 (0.29-23)	0.4
R2	0.68 (0.25-1.9)	
T cell infiltration (High)		
Low	1.5 (0.52-4)	0.5
Disease recurrence (No)[c]		
Yes	6.3 (0.83-48)	**0.04 ***

Recurrence-free survival[c]	Univariate		Multivariate	
Variable	**HR (95% CI)**	**log-rank *P***	**HR (95% CI)**	**log-rank *P***
Age at diagnosis	1 (0.98-1.02)	0.8		
Max tumour size	0.99 (0.9-1.1)	0.9		
Location (Skull base)[a]				
Mobile Spine	1.95 (0.94-4.02)	**0.003 ****	**2.2 (1-4.5) ***	
Sacrococcygeal	0.57 (0.26-1.2)		0.81 (0.32-2.1)	
Treatment (Surgery alone)				
Surgery + RT	0.82 (0.45-1.5)	0.5		**0.01 ***
Timing of RT (Adjuvant)[b]				
Neoadjuvant	0.29 (0.066-1.3)	0.08		
Surgical margin (R0)				
R1	1.6 (0.34-7.4)	0.07	1.2 (0.24-5.6)	
R2	**2.3 (1.1-4.8) ***		1.7 (0.7-4.2)	
T cell infiltration (High)				
Low	1.1 (0.6-2.1)	0.7		

[a]excluding the only patient with an extra-axial chordoma; [b]excluding patients who received a sandwich regimen of radiotherapy or radiotherapy alone; [c]excluding patients who were only treated with radiotherapy

Supplemental references

1. Bertucci F, Finetti P, Simeone I, Hendrickx W, Wang E, Marincola FM, et al. The immunologic constant of rejection classification refines the prognostic value of conventional prognostic signatures in breast cancer. Br J Cancer. 2018;119(11):1383-91.
2. Ijsselsteijn ME, van der Breggen R, Sarasqueta AF, Koning F, de Miranda NFCC. A 40-Marker Panel for High Dimensional Characterization of Cancer Immune Microenvironments by Imaging Mass Cytometry. Front Immunol. 2019;10.
3. Somarakis A, Van Unen V, Koning F, Lelieveldt B, Hollt T. ImaCytE: Visual Exploration of Cellular Micro-Environments for Imaging Mass Cytometry Data. IEEE Trans Vis Comput Graph. 2021;27(1):98-110.
4. Nelson AC, Pillay N, Henderson S, Presneau N, Tirabosco R, Halai D, et al. An integrated functional genomics approach identifies the regulatory network directed by brachyury (T) in chordoma. J Pathol. 2012;228(3):274-85.
5. Duan W, Zhang B, Li X, Chen W, Jia S, Xin Z, et al. Single-cell transcriptome profiling reveals intra-tumoral heterogeneity in human chordomas. Cancer Immunol Immunother. 2022;71(9):2185-95.
6. Zhang Q, Fei L, Han R, Huang R, Wang Y, Chen H, et al. Single-cell transcriptome reveals cellular hierarchies and guides p-EMT-targeted trial in skull base chordoma. Cell Discov. 2022;8(1):94.

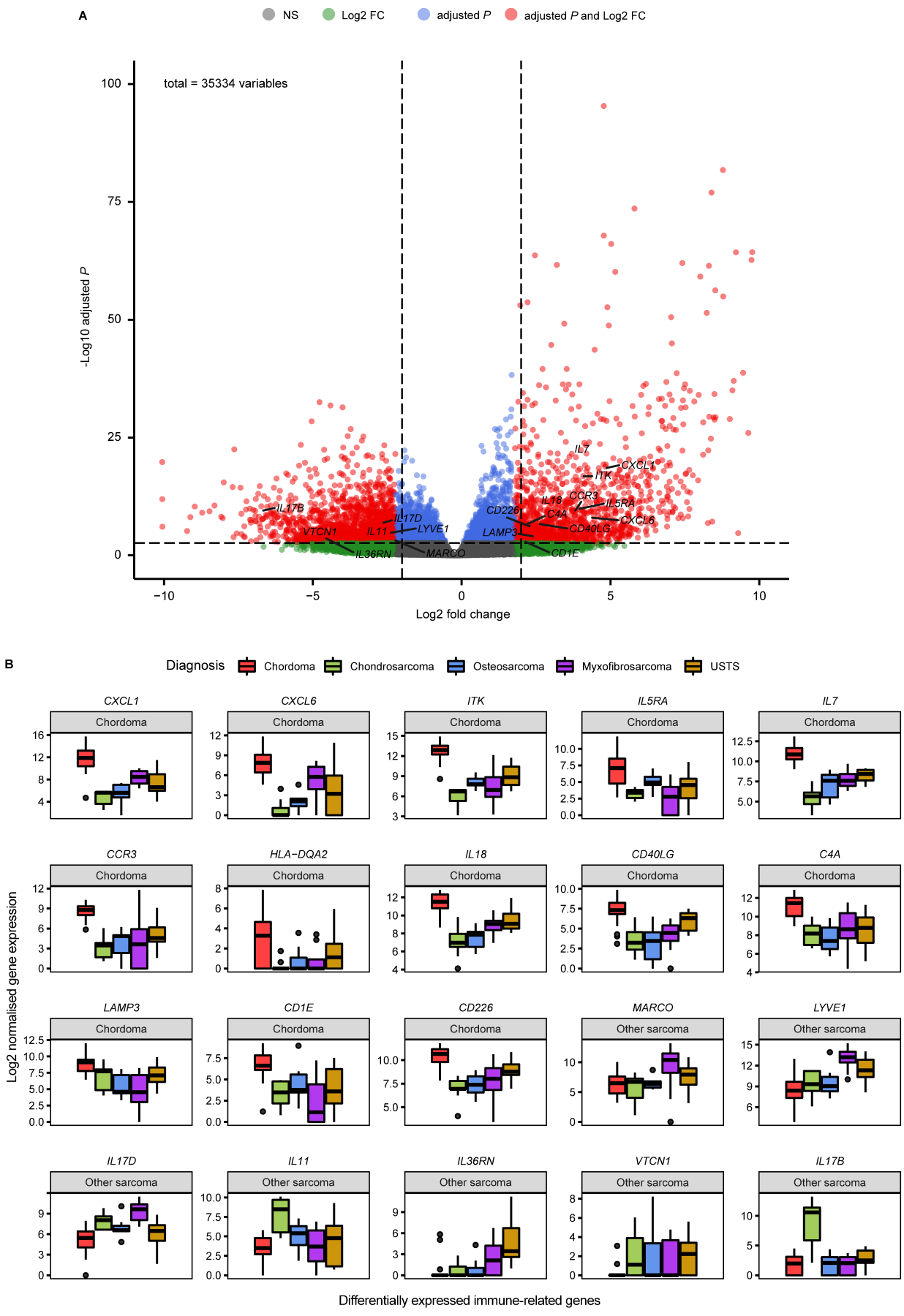
A
NS
Log2 FC
adjusted P
adjusted P and Log2 FC
total = 35334 variables
-Log10 adjusted P
Log2 fold change
B
Diagnosis
Chordoma
Chondrosarcoma
Osteosarcoma
Myxofibrosarcoma
USTS
Log2 normalised gene expression
Differentially expressed immune-related genes
CXCL1
CXCL6
ITK
IL5RA
IL7
CCR3
HLA−DQA2
IL18
CD40LG
C4A
LAMP3
CD1E
CD226
MARCO
LYVE1
IL17D
IL11
IL36RN
VTCN1
IL17B
Chordoma
Other sarcoma

Supplemental figure 1 | Chordomas are enriched for immune-related gene signaling. (A) Enhanced volcano plot presenting the differential gene expression analysis between chordomas (*n* = 20) and all other studied sarcomas (*n* = 39. Genes with a $\log_2$ fold change above 2 and an adjusted *P* value below 0.01 were considered significantly differentially expressed. Immune-related genes were labelled for visualisation. **(B)** Boxplots displaying the $\log_2$ normalised expression of the differentially expressed immune related genes. The boxplots are ordered in descending order for the $\log_2$ fold change and annotated for the respective group in which they are significanly enriched (chordoma vs other sarcoma). The boxplots are coloured for their respective histotype. NS = not significant; FC = fold change; USTS = undifferentiated soft tissue sarcoma.

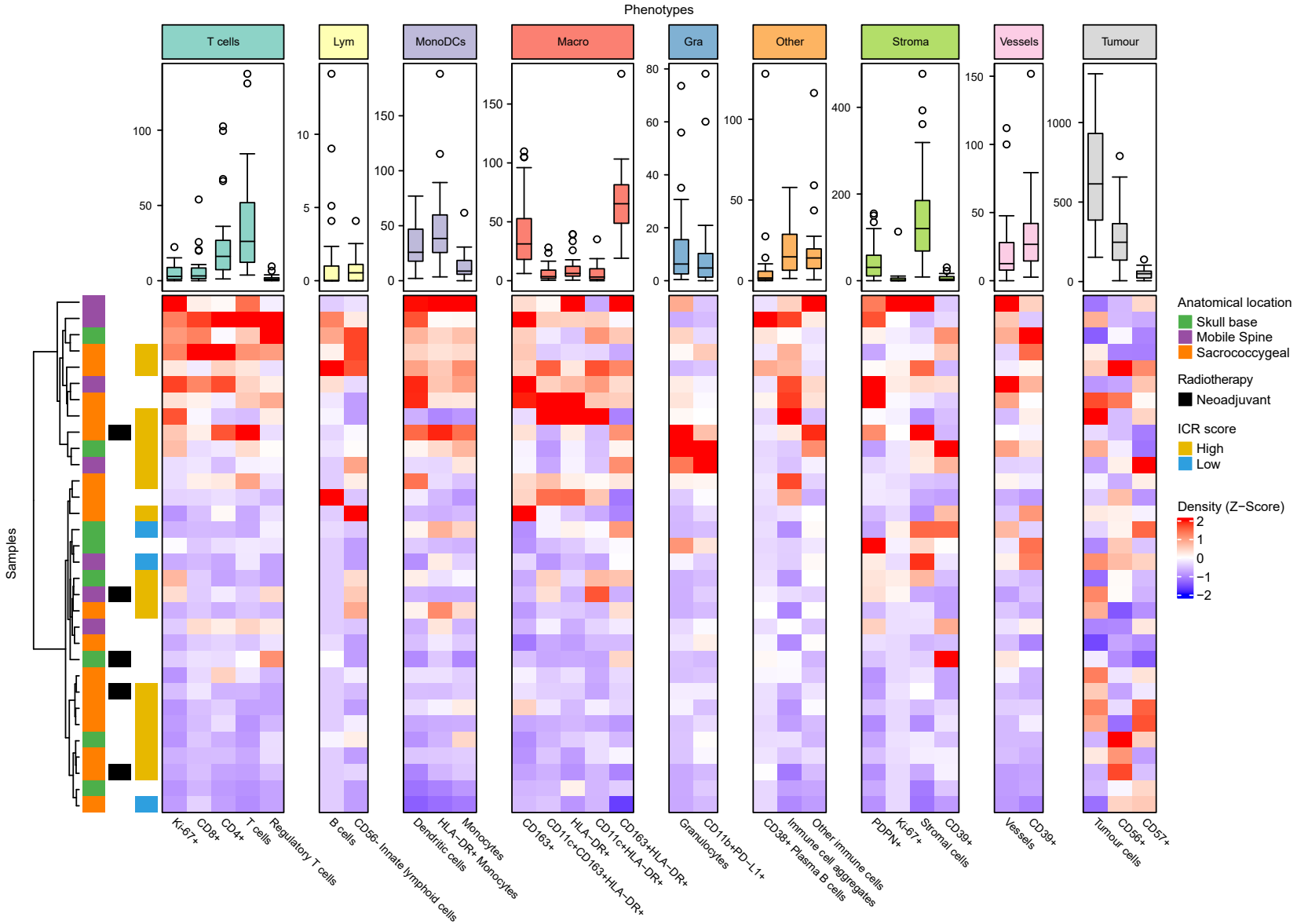
Phenotypes
T cells
Lym
MonoDCs
Macro
Gra
Other
Stroma
Vessels
Tumour
Samples
Ki-67+
CD8+
CD4+
T cells
Regulatory T cells
B cells
CD56- Innate lymphoid cells
Dendritic cells
HLA-DR+ Monocytes
Monocytes
CD163+
CD11c+CD163+HLA-DR+
HLA-DR+
CD11c+HLA-DR+
CD163+HLA-DR+
Granulocytes
CD11b+PD-L1+
CD38+ Plasma B cells
Immune cell aggregates
Other immune cells
PDPN+
Ki-67+
Stromal cells
CD39+
Vessels
CD39+
Tumour cells
CD56+
CD57+
Anatomical location
Skull base
Mobile Spine
Sacrococcygeal
Radiotherapy
Neoadjuvant
ICR score
High
Low
Density (Z−Score)
2
1
0
−1
−2

Supplemental figure 2 | Overview of the chordoma microenvironment. Overview heatmap of the mean cell density Z-Score of 29 identified cell phenotypes in all chordoma samples (*n* = 32). The samples that were used for transcriptome sequencing are annotated according to their ICR score. Samples are hierarchically clustered and annotated for their anatomical location and whether they had received neoadjuvant radiotherapy. Boxplots are presented per phenotype to display the general mean cell densities per mm^2 for each phenotype. ICR = immunologic constant of rejection; Lym = lymphoid; MonoDCs = monocytes and dendritic cells; Macro = macrophages; Gra = granulocytes; PDPN = podoplanin.

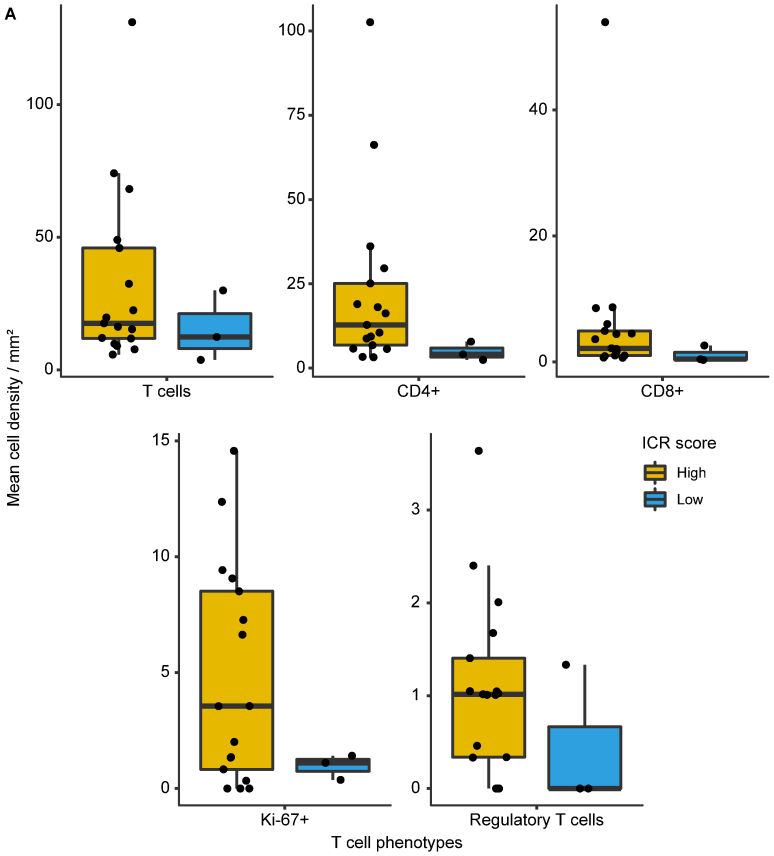
A
Mean cell density / mm²
T cells
CD4+
CD8+
Ki-67+
Regulatory T cells
T cell phenotypes
ICR score
High
Low

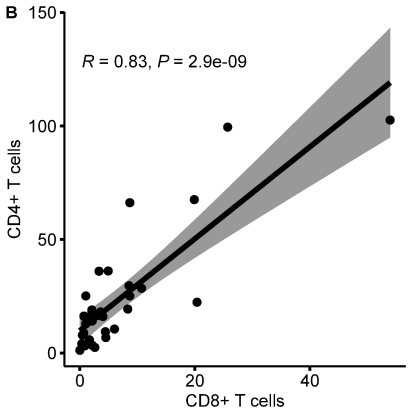
B
R = 0.83, P = 2.9e-09
CD4+ T cells
CD8+ T cells

Supplemental figure 3 | ICR high chordomas are enriched with T cell phenotypes. (A) Boxplots representing the different levels of infiltration of the identified T cell populations between ICR-high (*n* = 17) and ICR-low (*n* = 3) chordomas. No statistical tests were performed due to the small sample size. ICR = immunologic constant of rejection. **(B)** Correlation plot presenting the Pearson correlation between CD4+ T cell and CD8+ T cell infiltration based on the imaging mass cytometry data.

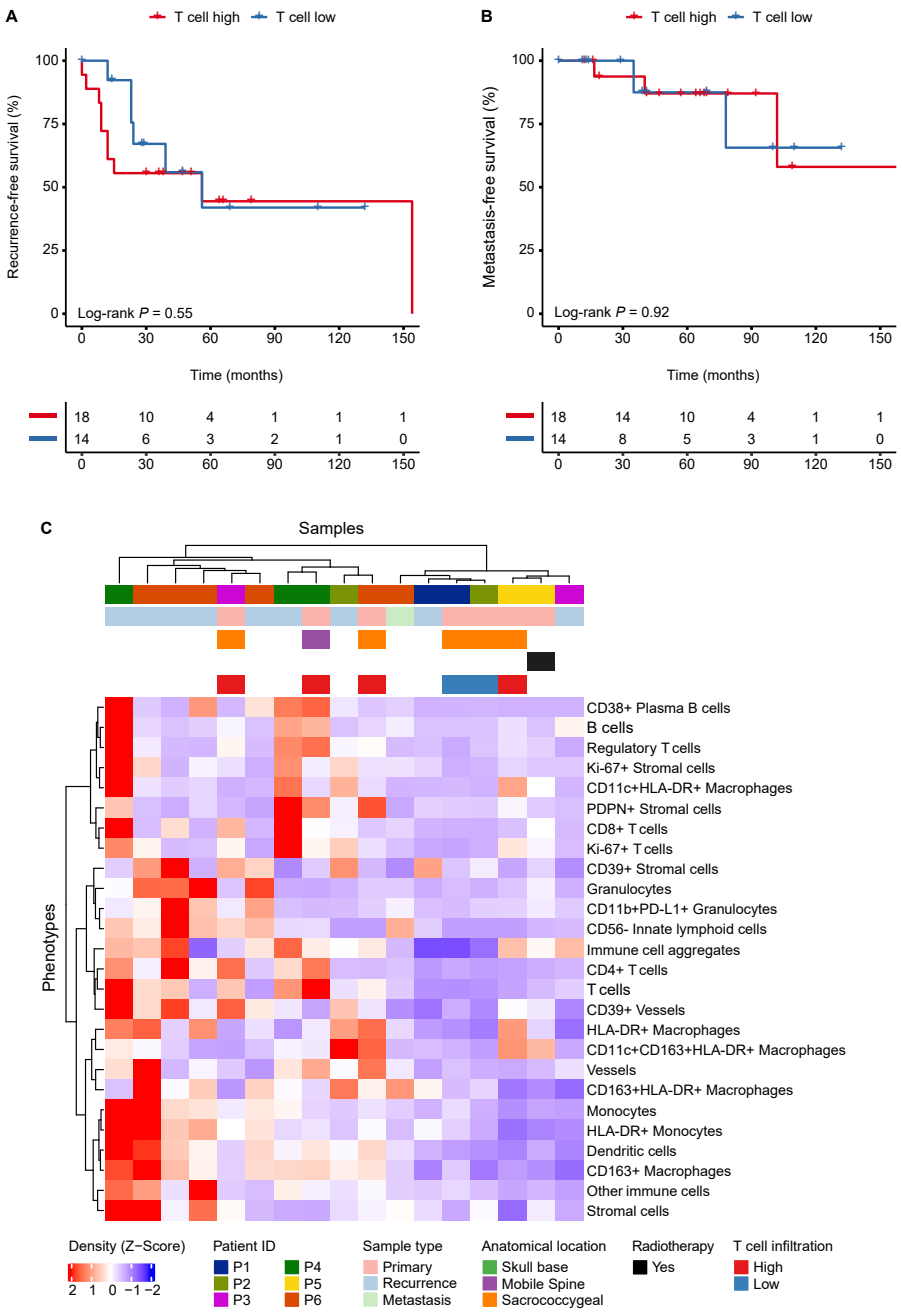
A
T cell high
T cell low
Recurrence-free survival (%)
Log-rank P = 0.55
Time (months)
B
Metastasis-free survival (%)
Log-rank P = 0.92
C
Samples
Phenotypes
CD38+ Plasma B cells
B cells
Regulatory T cells
Ki-67+ Stromal cells
CD11c+HLA-DR+ Macrophages
PDPN+ Stromal cells
CD8+ T cells
Ki-67+ T cells
CD39+ Stromal cells
Granulocytes
CD11b+PD-L1+ Granulocytes
CD56- Innate lymphoid cells
Immune cell aggregates
CD4+ T cells
T cells
CD39+ Vessels
HLA-DR+ Macrophages
CD11c+CD163+HLA-DR+ Macrophages
Vessels
CD163+HLA-DR+ Macrophages
Monocytes
HLA-DR+ Monocytes
Dendritic cells
CD163+ Macrophages
Other immune cells
Stromal cells
Density (Z−Score)
Patient ID
P1
P2
P3
P4
P5
P6
Sample type
Primary
Recurrence
Metastasis
Anatomical location
Skull base
Mobile Spine
Sacrococcygeal
Radiotherapy
Yes
T cell infiltration
High
Low

Supplemental figure 4 | The immune contexture of chordomas varies over time. (A, B) Kaplan-Meier curve indicating the association between T cell infiltration and recurrence-free survival **(A)** as well as metastasis-free survival **(B)**. Two-sided log-rank tests were performed for the Kaplan Meier estimates. **(C)** Heatmap presenting the unsupervised clustering of untreated primary tumours (*n* = 6) and their respective treated primary tumour (*n* = 1), recurrences (*n* = 9) and metastases (*n* = 1). The heatmap displays the mean cell density Z-Score of the identified cell phenotypes, excluding tumour cells. The samples are annotated for patient ID, type of sample, anatomical location, whether the tumour was treated with neoadjuvant radiotherapy and T cell group of the primary tumour. PDPN = podoplanin.

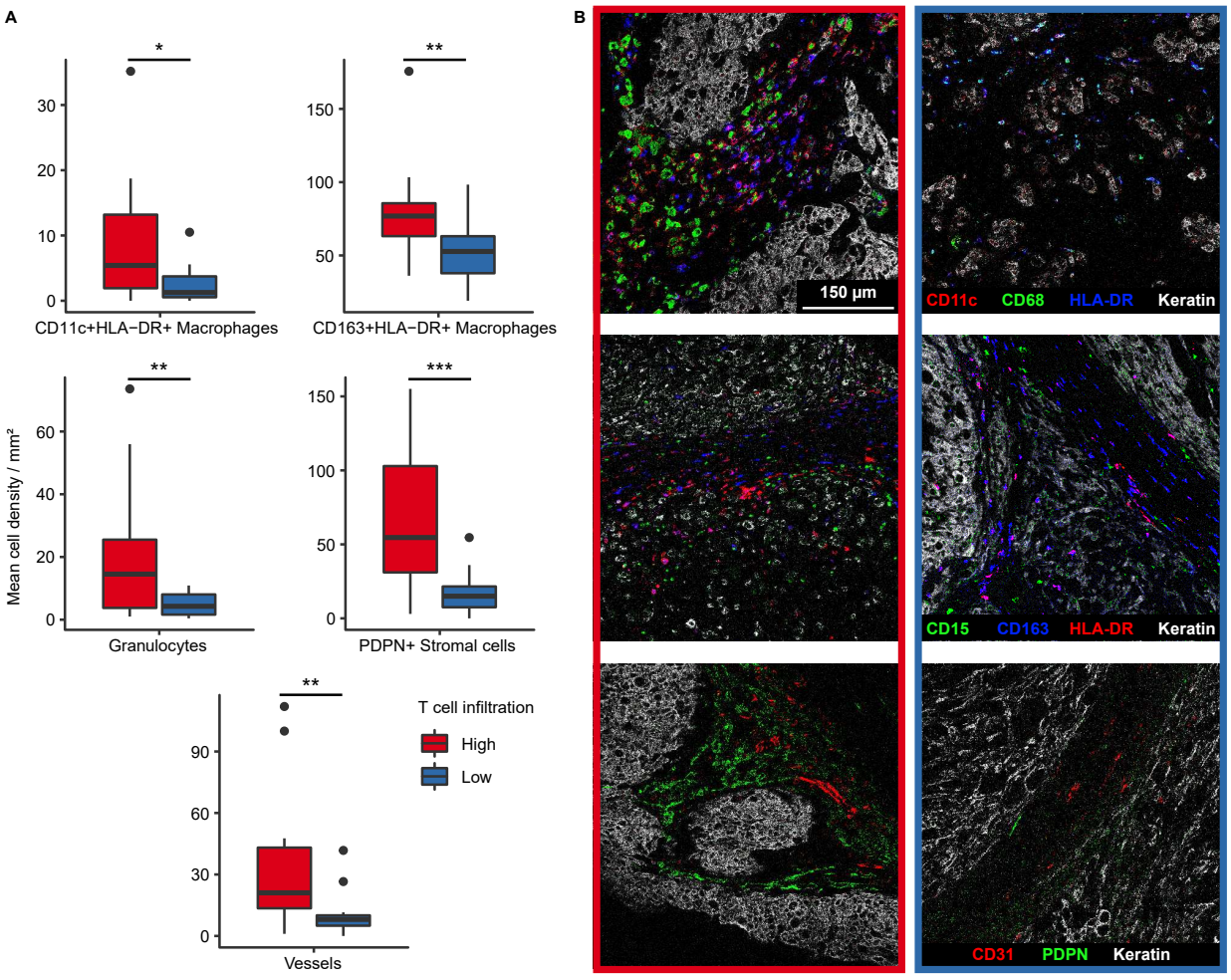
A
B
CD11c+HLA−DR+ Macrophages
CD163+HLA−DR+ Macrophages
Granulocytes
PDPN+ Stromal cells
Vessels
Mean cell density / mm²
T cell infiltration
High
Low
150 µm
CD11c CD68 HLA-DR Keratin
CD15 CD163 HLA-DR Keratin
CD31 PDPN Keratin

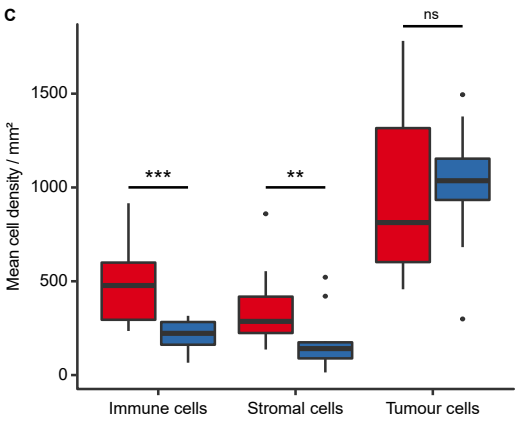
C
Mean cell density / mm²
Immune cells
Stromal cells
Tumour cells
ns

Supplemental figure 5 | Comparative overview of the chordoma immune microenvironment. (A) Boxplots with the significantly different phenotypes between the T cell high and T cell low groups. Two-sided t-test was performed in R and the *P* value was adjusted with the Benjamini-Hochberg false discovery rate (FDR). All presented phenotypes were significantly different between the T cell high an T cell low group. * = $P < 0.05$; ** = $P < 0.01$; *** $P < 0.001$. **(B)** Representative images generated with imaging mass cytometry displaying the differentially abundant cell phenotypes in both T cell low and T cell high samples. Images are grouped per row for the displayed cell markers and outlined with their respective T cell group (T cell high = red rectangle & left, T cell low = blue rectangle & right). The top row presents $CD11c^+$ macrophages (CD11c = red, CD68 = green, HLA-DR = blue, keratin = white), the middle row displays granulocytes and $CD163^+$HLA-DR+ macrophages (CD15 = green, CD163 = blue, HLA-DR = red, keratin = white) and the bottom row shows vessels and $podoplanin^+$ stromal cells (CD31 = red, PDPN = green, keratin = white). **(C)** Boxplots presenting the cumulative mean cell density per mm^2 of all immune cells, stromal cells and tumour cells in both T cell high and T cell low groups. Two-sided t-test was performed in R. ** = $P < 0.01$, *** = $P < 0.001$. PDPN = podoplanin.

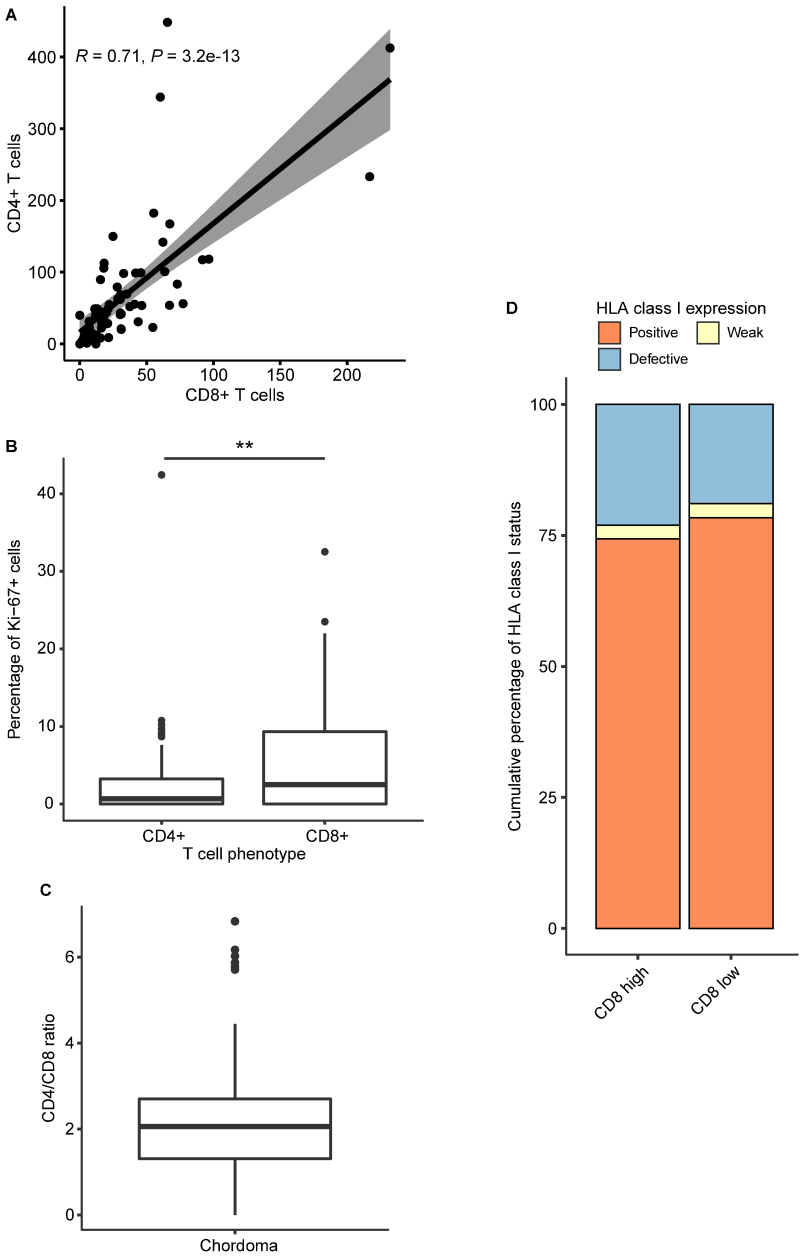
A
R = 0.71, P = 3.2e-13
CD4+ T cells
CD8+ T cells
B
**
Percentage of Ki−67+ cells
CD4+
CD8+
T cell phenotype
C
CD4/CD8 ratio
Chordoma
D
HLA class I expression
Positive
Weak
Defective
Cumulative percentage of HLA class I status
CD8 high
CD8 low

Supplemental figure 6 | CD4+ T cell infiltration and HLA class I expression in association with CD8+ T cell infiltration. (A) Correlation plot presenting the Pearson correlation between CD4+ T cell and CD8+ T cell infiltration based on the immunofluorescence data. **(B)** Boxplots displaying the percentage of Ki-67+ cells for CD4+ and CD8+ T cells. A two-sided t-test was performed to compare Ki-67+CD4+ T cells with Ki-67+CD8+ T cells. ** = $P < 0.01$. **(C)** Boxplot presenting the CD4/CD8 ratio in chordomas **(D)** Stacked bar plots displaying the percentual distribution of the observed HLA class I (both HCA2 and HC10) expression patterns in the chordoma samples divided into CD8+ T cell high and low with the median cell density as cut-off. (CD8+ high: $n = 37$; CD8+ low: $n = 37$).

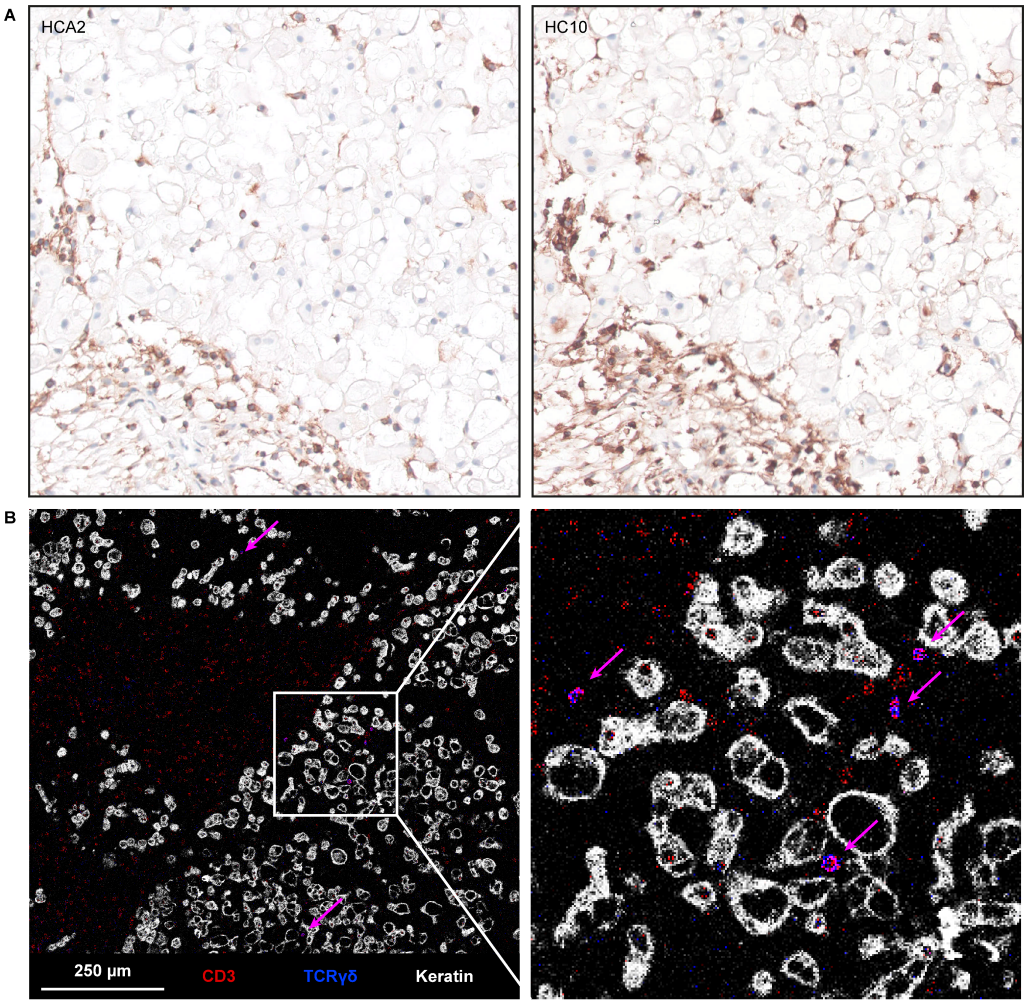
A
HCA2
HC10
B
250 µm
CD3
TCRγδ
Keratin

Supplemental figure 7 | γδ T cell infiltration in relation to HLA class I expression. (A) Examples images of Human Leukocyte Antigen (HLA) class I (HCA2 and HC10) expression in a T cell high chordoma as validated by immunohistochemistry. **(B)** An example image and a corresponding magnification of the same tissue core as displayed in **(A)** as generated by imaging mass cytometry. The images present intratumoral γδ T cell infiltration as indicated by the magenta arrows (CD3 = red, TCRγδ = blue, keratin = white). TCR = T cell receptor.